# SUPPLEMENTAL MATERIALS

## Synthesis and Preclinical Evaluation of $^{11}$C-UCB-J as a PET Tracer for Imaging the Synaptic Vesicle Glycoprotein 2A in the Brain

Nabeel B Nabulsi[1]*, Joël Mercier[2]*, Daniel Holden[1], Stephane Carré[2], Soheila Najafzadeh[1], Marie-Christine Vandergeten[2], Shu-fei Lin[1], Anand Deo[2], Nathalie Price[2], Martyn Wood[2], Teresa Lara-Jaime[1], Florian Montel[2], Marc Laruelle[3], Richard E. Carson[1], Jonas Hannestad[2], Yiyun Huang[1]

*Shared first authors

[1]Yale PET Center, New Haven, CT, USA

[2]UCB Biopharma, Braine-l'Alleud, Belgium

[3]Intracellular Therapeutics, New York, NY, USA

CONTENT

**Chemistry**

I. Synthesis of UCB-J reference standard **3** is depicted in Supplemental Scheme 1 (*1*):

Supplemental Scheme 1

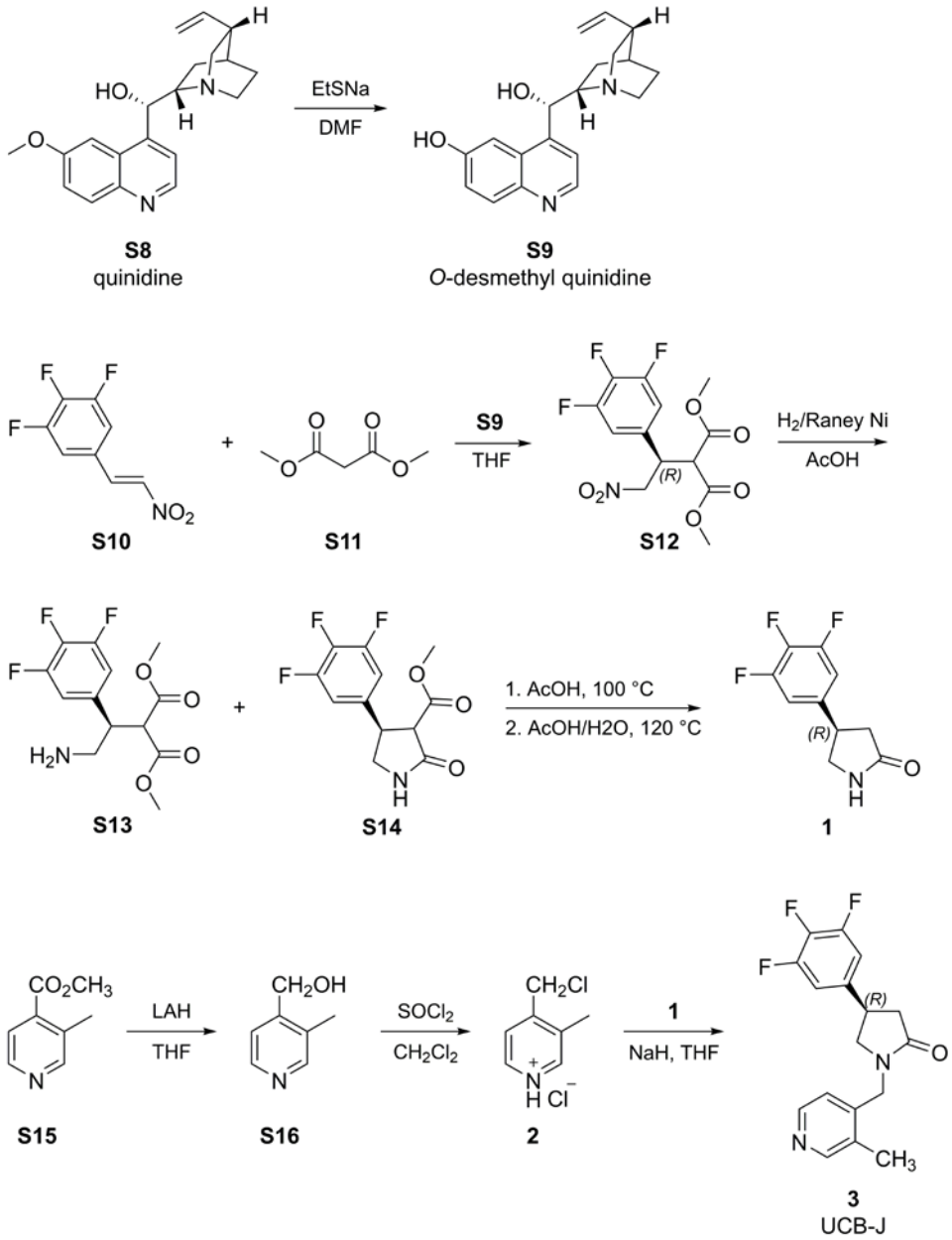

**Preparation of the *O*-desmethyl quinidine catalyst: 4-((*S*)-hydroxy-((1*S*,2*S*,4*S*,5*R*)-5-vinylquinuclidin-2-yl)methyl)quinolin-6-ol (S9)**:

In a 250 ml reaction flask under nitrogen, quinidine **S8** (10g, 30.8 mmoles) and sodium ethanethiolate (7.8 g, 92.7 mmoles) were dissolved in DMF (50 ml). The reaction mixture was heated overnight at 115°C. After cooling to room temperature, isopropyl alcohol (50 ml) was added followed by dropwise addition of aqueous ammonium chloride (110 ml, 14% w/w in water). The reaction mixture was maintained at room temperature during the course of the addition and stirring was continued for 3-4 hours. The precipitate was filtered, washed twice with water (2 × 15 ml) and with isopropyl alcohol (1 × 25 ml) and dried under vacuum, giving 7.5 g (yield = 78%) of catalyst **S9**. $^1$H NMR (400 MHz, $CD_3OD$): δ 8.60 (d, 1 H, J = 4.1 Hz), 7.91 (d, 1 H, J = 9.0 Hz), 7.65 (d, 1 H, J = 3.9 Hz), 7.31 (m, 2 H), 6.18 (m, 1 H), 5.62 (s, 1 H), 5.11 (m, 2 H), 3.64 (m, 1 H), 3.33 (s, 1 H), 2.92 (m, 4 H), 2.27 (m, 2 H), 1.74 (s, 1 H), 1.57 (m, 2 H), 1.01 (m, 2 H).

**Dimethyl (*R*)-2-(2-nitro-1-(3,4,5-trifluorophenyl)ethyl)malonate (S12)**:

In a 2 L reaction flask under nitrogen, nitrostyrene **S10** (245 g, 1.206 moles) and dimethyl malonate **S11** (207 g, 1.568 moles, 1.3 eq.) were dissolved in THF (1225 ml). After cooling to -20 °C, a suspension of the catalyst **S9** (7.5 g, 24.1 mmoles, 0.02 eq) in THF (40 ml) was added. Stirring was maintained at -20 °C for ~24 h. THF was removed at 50 °C under slight vacuum and replaced by n-butanol (1350 ml). The alcoholic phase was diluted with water (540 ml), brought again to 50 °C and then slowly cooled to 35 °C overnight so that a precipitate is obtained. The mixture was further cooled to 5 °C and the resulting precipitate was filtered, washed with a n-butanol/water mixture (250 ml, 70% n-butanol/30% water) and dried under vacuum giving 313 g (yield = 77%) of **S12** as white

crystals. $^1$H NMR (400 MHz, CDCl3): δ 6.92 (m, 2 H), 4.86 (m, 2 H), 4.19 (m, 1 H), 3.79 (m, 4 H), 3.66 (s, 3 H).

**(4*R*)-4-(3,4,5-trifluorophenyl)pyrrolidin-2-one (1)**:

The nitro intermediate **S12** (14.2 kg, 42.4 moles) was dissolved in acetic acid (43 L) in a 250 L reactor, and the resulting solution was stirred for 15 minutes under nitrogen. The solution was then transferred under nitrogen atmosphere to a 200 L stainless steel hydrogenation reactor charged with Raney Ni (1.4 kg, 10% W/W). The reactor was purged 5 times with hydrogen, then filled to 4 bars, then hydrogenated at 45° C for 5 hours. After complete conversion of the nitro intermediate, hydrogen was removed, and the mixture was cooled to room temperature and filtered, affording after concentration 84 kg of a 15% W/W solution of a ~75/25 mixture of compounds **S13** and **S14**.

In a 2 L reactor, 2.015 kg of the above solution was heated at 98 ° C during 1 h to complete the cyclization into intermediate **S14**. Water was then added (~70 ml, 1 g per 25 g acetic acid). The reactor was fitted with a distillation head and the mixture was brought to 120 ° C during ~ 36 hours to complete the hydrolysis/decarboxylation, during which about 52 g of a colorless liquid (mostly methyl acetate) was distilled off. The crude mixture was cooled to room temperature and then filtered to remove the precipitate. The volume of the resulting filtrate was concentrated to ~500 ml by removing acetic acid through distillation. Water (~1320 ml) was added to the resulting concentrated solution at 60°C, then the temperature was decreased to 20 °C. The resulting precipitate was filtered and dried, giving **1** as a light brown solid (171.6 g, yield = 78% from **S12**) of 97.6% ee; $[\alpha]_D$ -17.6 (MeOH, 22°C); $^1$H NMR (400 MHz, DMSO): δ 7.71 (s, 1 H), 7.30 (dd, 2 H, J = 9.1, 7.0 Hz), 3.57 (m, 2 H), 3.15 (t, 1 H, J = 8.2 Hz), 2.42 (m, 1 H), 2.31 (dd, 1 H, J =

16.3, 9.5 Hz). Chiral LC: Chiralpak AS-H, 5 µm, 250 × 4.6 mm, 50% ethanol/50% n-heptane/0.1% DEA, T = 30 °C, flow rate 1 ml/min. **S12** *(R)*-enantiomer $t_R$ = 7.5 min; *(S)*-enantiomer $t_R$ = 11.9 min (Supplemental Fig. 1).

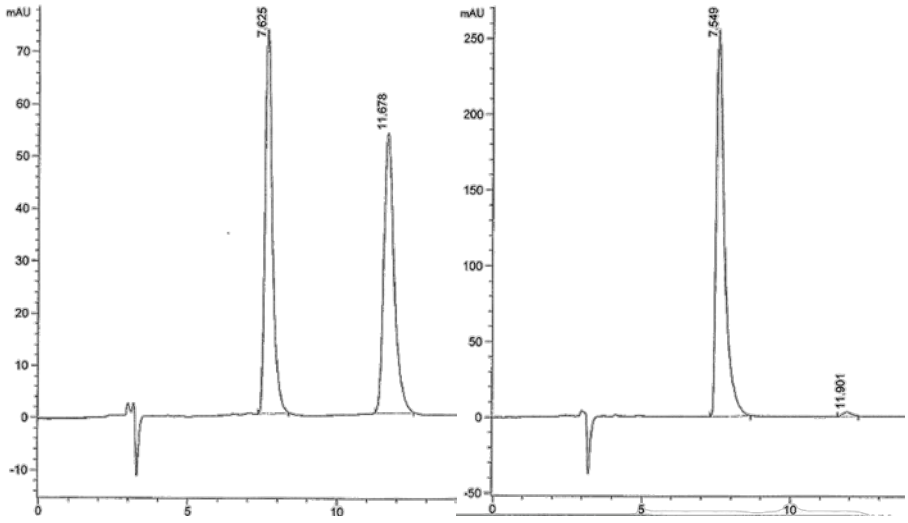


Supplemental Figure 1. Left: chiral chromatogram of the racemate of intermediate **1** ; Right : chiral chromatogram of the (*R*)-enantiomer used in the reported studies (ee= 97.6%)

**3-Methyl-4-(pyridyl)methanol (S16)**:

Under nitrogen, 10 g (66.0 mmol) of methyl 3-methyl-4-pyridinecaboxylate **S15** was dissolved in 150 mL of dry THF in a 1 L 3-necked round-bottom flask. After the solution was cooled to 0 °C, 3 g (1.2 equiv., 79.4 mmol) of lithium aluminium hydride was added in small portions. The resulting reaction mixture was stirred at room temperature overnight. After completion of the reaction, 10 mL of water was added to the mixture, followed by 4 spoons of sodium sulphate. The reaction mixture was then filtered over celite. Removal of the solvent under reduced pressure gave **S16** (8 g) as a yellow solid which was used in the next step without further purification. LC-MS: *m/z* [$MH^+$] = 124.2

**3-Methyl-4-(chloromethyl)pyridine hydrochloride (2)**:

Under nitrogen, 8 g (65.0 mmol) of (3-methyl-4-pyridyl)methanol **S16** was dissolved in 100 mL of dichloromethane in a 1 L round-bottom flask. After cooling the solution to 0 °C, 9.3 g (1.2 equiv., 78.0 mmol) of thionyl chloride was added dropwise, and then the reaction mixture was further stirred at room temperature upon completion of the reaction. Removal of the solvent under reduced pressure gave **2** (11 g) as a yellow solid which was used in the next step without further purification. LC-MS: *m/z* [$MH^+$] = 142/144.

**(4*R*)-1-[(3-methyl-4-pyridyl)methyl]-4-(3,4,5-trifluorophenyl)pyrrolidin-2-one (UCB-J) (3)**:

In a 3-necked round-bottom flask, (4*R*)-4-(3,4,5-trifluorophenyl)pyrrolidin-2-one **1** (13 g, 60.417 mmol) was added to a solution of 3-mehyl-4-(chloromethyl)pyridine hydrochloride **2** (10.758 g, 60.417 mmol, 1 eq) and potassium iodide (1.003 g, 6.0417 mmol, 0.1 eq) in THF (300 ml). After cooling to 0 °C, sodium hydride, 60% dispersion in oil (4.579 g, 181.25 mmol, 3 eq.) was added in small portions. Then the reaction mixture was stirred for 2 h at 50 °C. A second portion of sodium hydride (2.3 g, 92 mmol, 1.5 eq.) was added to achieve complete conversion of the pyrrolidinone. The reaction mixture was quenched with saturated aqueous $NaHCO_3$, and THF was removed under reduced pressure. The resulting crude solid was then dissolved in ethyl acetate (500 ml) and brine (500 ml). The organic layer was separated, washed twice with brine, dried over $Na_2SO_4$, and then concentrated under vacuum. The crude product was purified by silica gel liquid chromatography ($CH_2Cl_2$/MeOH/$NH_4OH$ 95/ 5/0.5 v /v/v) affording an off-white solid which was suspended in a 1/ 1 mixture of ethyl acetate/diethyl ether. The solid was filtered and dried under vacuum to give (4*R*)-1-[(3-methyl-4-pyridyl)methyl]-4-(3,4,5-trifluorophenyl)pyrrolidin-2-one (UCB-J) **3** (12.5g, yield 65%) as a white powder with

melting point of 115.3 °C, and purity of 99.4% by HPLC, 99% by $^{1}$H-NMR, and 99.1% ee by chiral HPLC; $[\alpha]_D$ + 31.7 (MeOH, 22°C); $^{1}$H NMR (400 MHz, DMSO) δ 8.38 (s, 2 H), 7.34 (dd, 2 H, *J* = 9.1, 7.0 Hz), 7.16 (d, 1 H, *J* = 4.9 Hz), 4.55 (d, 1 H, *J* = 16.0 Hz), 4.35 (d, 1 H, *J* = 16.0 Hz), 3.70 (m, 1 H), 3.61 (t, 1 H), 3.26 (t, 1 H, *J* = 8.4 Hz), 2.75 (dd, 1 H, *J* = 16.4, 8.6 Hz), 2.61 (dd, 1 H, *J* = 16.3, 9.3 Hz), 2.26 (s, 3 H). HRMS (ES+,TOF) *m/z* calculated for $[M + H]^+$ $C_{17}H_{16}F_3N_2O$ 321.1209, found 321.1222. Chiral LC: method A; Chiralpak AD-H, 5 µm, 250 × 4.6 mm, 50% ethanol/50% n-heptane/0.1% DEA, T = 30 °C, flow rate 1 ml/min. UCB-J $t_R$ = 6.6 min; *(S)*-enantiomer $t_R$ = 5.4 min; method B (Supplemental Fig. 2); Chiralcel OD, 250 × 4.6 mm, 75 heptane/25 ethanol/0.1 triethylamine, flow rate 2 mL/min at 254 nm.

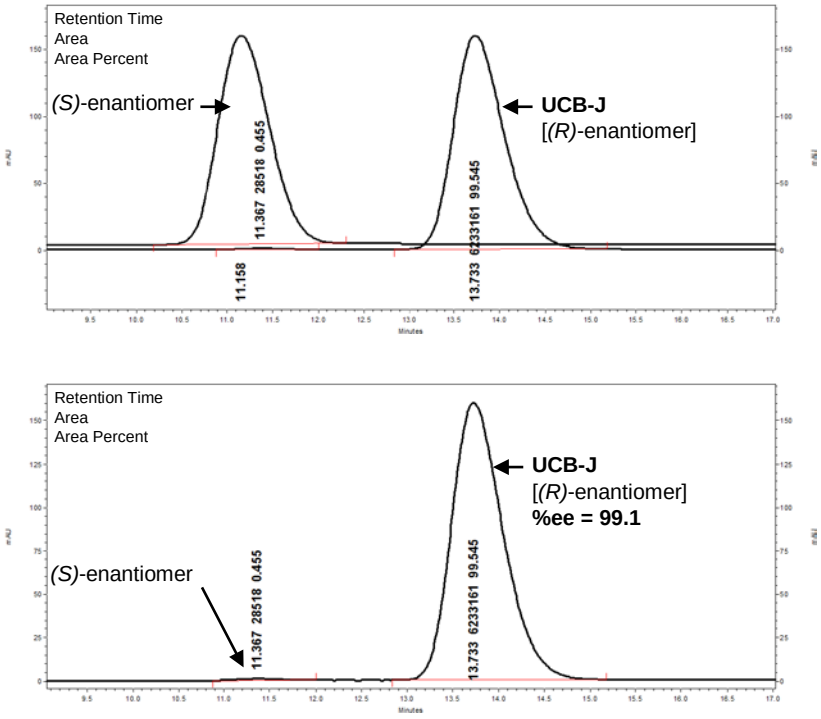


Supplemental Figure 2. Method B chiral HPLC chromatograms.

II. Synthesis of the trifluoroborate radiolabeling precursor is outlined in Supplemental Scheme 2.

Supplemental Scheme 2

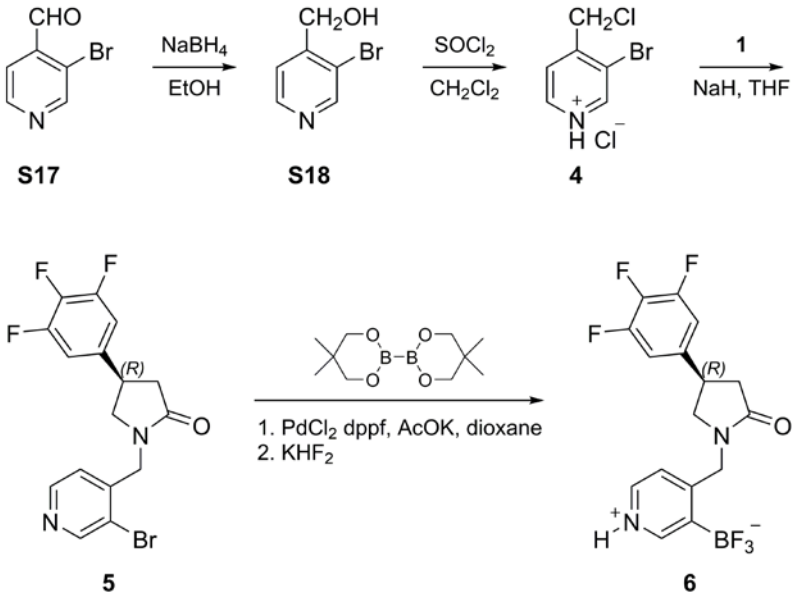


**3-Bromo-4-(pyridyl)methanol (S18)**:

Under nitrogen, $NaBH_4$ (5.48 g, 143.3 mmol, 1.1 eq.) was added at room temperature to a 1 L round-bottom flask containing a solution of 3-bromo-4-pyridinecarboxadehyde **S17** (25 g, 130.4 mmol, 1eq.) in EtOH (300 ml). The reaction mixture was stirred for 48 h at room temperature and then quenched with water (200 ml) and diluted with ethyl acetate (500 ml). The organic layer was extracted, washed with brine and dried over anhydrous $MgSO_4$. Evaporation of the solvent under vacuum gave 19.65 g of crude alcohol **S18** which was used in the next step without further purification. $^1$H NMR (400 MHz, DMSO) δ 8.63 (s, 1 H), 8.55 (d, 1 H, J = 4.9 Hz), 7.55 (d, 1 H, J = 4.8 Hz), 5.68 (t, 1 H, J = 5.6 Hz), 4.53 (d, 2 H, J = 5.5 Hz).

**3-Bromo-4-(chloromethyl)pyridine hydrochloride (4)**:

Under nitrogen, thionyl chloride (9.9 ml, 140 mmol, 1.3 eq.) was added dropwise to a 1 L round-bottom flask containing a solution of 3-bromo-4-(pyridyl)methanol **S18** (19.65 g, 104.5 mmol, 1 eq.) in dichloromethane (200 ml) at 0°C. The reaction mixture was further stirred at room temperature upon completion. Removal of the solvent under reduced pressure yielded 25.35 g of **4**. $^1$H NMR (400 MHz, DMSO) δ 8.79 (m, 1 H), 8.60 (m, 1 H), 7.68 (m, 1 H), 4.78 (m, 2 H).

**(4*R*)-1-[(3-bromo-4-pyridyl)methyl]-4-(3,4,5-trifluorophenyl)pyrrolidin-2-one (5)**:

In a 3-necked round-bottom flask, (4*R*)-4-(3,4,5-trifluorophenyl)pyrrolidin-2-one **1** (19 g, 88.302 mmol, 1 eq) was added to a solution of 3-bromo-4-(chloromethyl)pyridine hydrochloride **4** (25.35 g, 105.96 mmol, 1.2 eq.) in THF (500 ml). After cooling to 0 °C, sodium hydride, 60% dispersion in oil (10.59 g, 264.9 mmol, 3 eq.) was added in small portions and the reaction mixture was stirred overnight at 50 °C until complete conversion of the pyrrolidinone **1**. The reaction mixture was then diluted with ethyl acetate (500 ml), brine (500 ml), followed by addition of charcoal, and the resulting mixture was filtered through celite. The organic layer was extracted with ethyl acetate, then washed twice with brine and dried over $MgSO_4$ and then concentrated under vacuum. The resulting crude product was purified twice by silica gel liquid chromatography ($CH_2Cl_2$/MeOH/$NH_4OH$ 97.8/2/0.2 v/v/v) to afford (4*R*)-1-[(3-bromo-4-pyridyl)methyl]-4-(3,4,5-trifluorophenyl)pyrrolidin-2-one **5** (13.5 g, yield 40%) of 94.06% ee; $[\alpha]_D$ +27.71 (MeOH, 22°C); $^1$H NMR (400 MHz, DMSO) δ 8.73 (s, 1 H), 8.53 (d, 1 H, J = 4.9 Hz), 7.36 (m, 3 H), 4.57 (d, 1 H, J = 16.6 Hz), 4.40 (d, 1 H, J = 16.7

Hz), 3.72 (m, 2 H), 2.75 (dd, 1 H, J = 16.5, 8.4 Hz), 2.61 (dd, 1 H, J = 16.4, 9.3 Hz). HRMS (ES+,TOF): *m/z* calculated for $[M + H]^+$ $C_{16}H_{12}BrF_3N_2O$, 385.0163; found, 385.0165. Chiral LC: Chiralpak AD-H, 5 µm, 250 × 4.6 mm; 50% n-PrOH/50% n-heptane/0.1% DEA, T = 30 °C, flow rate 1 ml/min. (*R*)-enantiomer $t_R$ = 6.6 min; (*S*)-enantiomer $t_R$ = 5 min (Supplemental Fig. 3).

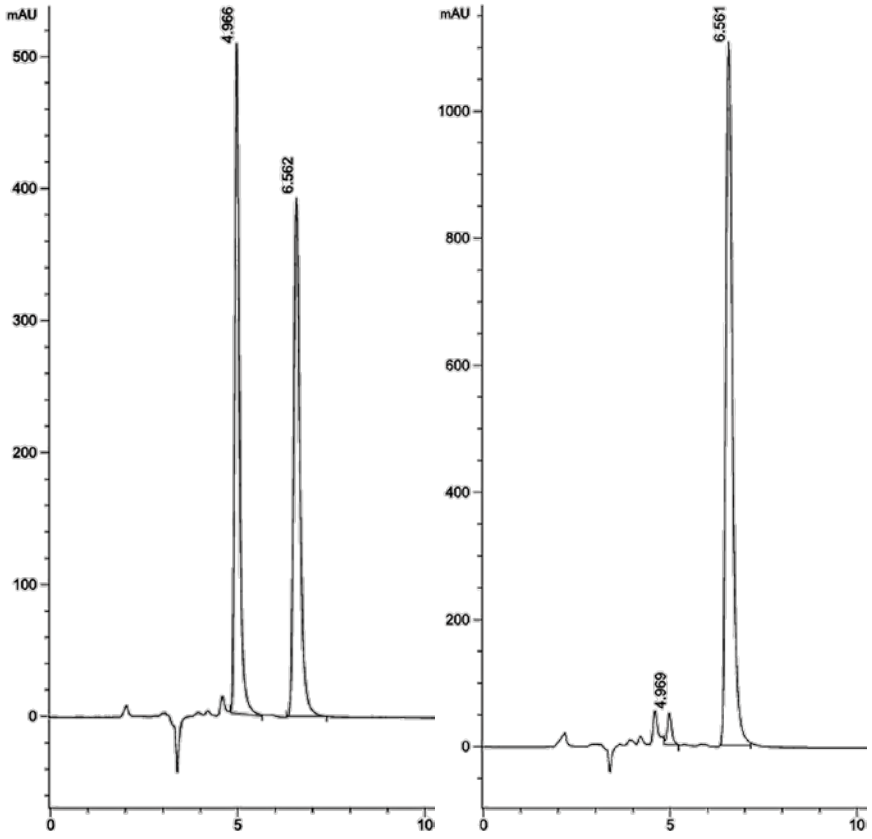


**Supplemental Figure 3**. Left: chiral chromatogram of the racemate of intermediate **5** ; Right : chiral chromatogram of the (*R*)-enantiomer used in the reported studies (ee= 94.06%)

**(*R*)-3-(difluoroboranyl)-4-((2-oxo-4-(3,4,5-trifluorophenyl)pyrrolidin-1-l)methyl)-pyridin-1-ium fluoride (6)**:

The pyrrolidinone **5** (5 g, 12.98 mmol), bis(neopentylglycato)diboron (6.59 g, 25.96 mmol), potassium acetate (3.86 g, 38.94 mmol), and $Pd(dppf)Cl_2$ (0.475 g, 0.65 mmol) were added to a 250 mL 3-necked round-bottomed flask. This mixture of solids was stirred under nitrogen for 10 min. Dioxane (103.3 g, 1,172 mmol), flushed with nitrogen for 10 min, was added to the mixture of solids, and the solution was heated at 110 °C for 4 h. The reaction was monitored by thin-layer chromatography (ethyl acetate/methanol 9:1) until complete conversion of compound **5**. The mixture was then quenched with ethyl acetate (350 mL) and brine (350 mL). The organic layer was separated, and the aqueous phase was extracted a second time with ethyl acetate (175 mL). Bone charcoal was added to the combined organic phases, and the mixture was heated to 40 °C and stirred additional 20 min, then filtered over celite previously washed with ethyl acetate (50 mL). Hydrochloric acid (280 mL, 1 M) was added to the combined filtrate and the solution was stirred for 45 min. The organic layer was separated and washed again with 1 M hydrochloric acid (210 mL). $KHF_2$ (4.1 g, 52 mmol) was added to the combined aqueous phases and the mixture was stirred at room temperature overnight. The aqueous phase was extracted twice with ethyl acetate (350 mL). The combined organic phases was washed with 1 M hydrochloric acid (350 mL) and brine (350 mL). The organic phase was dried over $MgSO_4$ and concentrated under vacuum at ambient temperature. The solid was suspended in diethyl ether, filtered and dried under vacuum to afford **6** (2.05 g, 42%) as an off-white powder with melting point 240-243 °C (dec), and 97% chemical purity by HPLC. $[\alpha]_D$ +25.35 (MeOH, 22°C); $^1$H NMR (400 MHz, DMSO) δ 14.94 (broad, 1H),

8.62 (d, 1 H, *J* = 6.1 Hz), 8.46 (s, 1 H), 7.65 (d, 1 H, *J* = 6.1 Hz), 7.38 (dd, 2 H, *J* = 9.2, 6.8 Hz), 4.85 (d, 1 H, *J* = 17.9 Hz), 4.70 (d, 1 H, *J* = 17.9 Hz), 3.74 (m, 2 H), 2.76 (dd, 1 H, *J* = 16.3, 8.5 Hz), 2.64 (dd, 1 H, *J* = 16.3, 9.6 Hz). HRMS (ES+, TOF): *m/z* calculated for $[M - HF]^+$ $C_{16}H_{11}BF_5N_2O$ 355.1041, found 355.1049; *(m/z)* calculated for $[M - H]^-$ $C_{16}H_{12}BF_6N_2O$ 373.0947; found, 373.0947.

**Radiochemistry**

**(*R*)-1-((3-(methyl-$^{11}$C)pyridin-4-yl)methyl)-4-(3,4,5-trifluorophenyl)pyrrolidin-2-one ($^{11}$C-UCB-J) (7)**

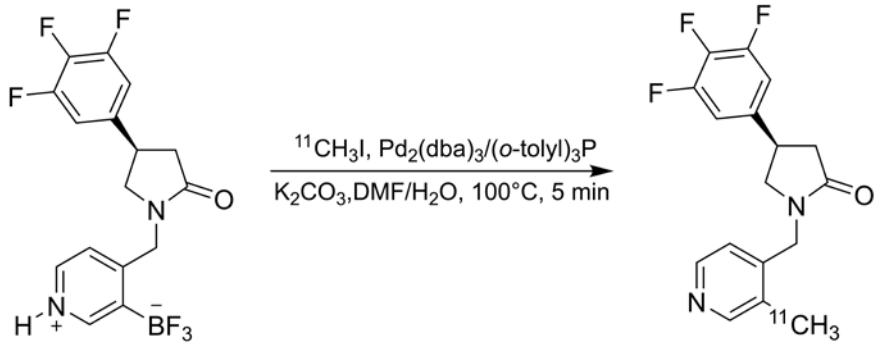


**6** **7**
$^{11}$C-UCB-J

The following radio-HPLC systems were used: a preparative HPLC system including a Shimadzu LC-20A pump, a Rheodyne 7133i injector with a 2-mL loop, a Knauer K200 ultraviolet detector, a Bioscan γ-flow detector, and a laptop computer running the EZStart data acquisition software; an analytic HPLC system consisting of a Shimadzu LC-20A quaternary pump, a Rheodyne 7133i injector, a Shimadzu SPD-M20A PDA or SPD-20A

ultraviolet detector, a flow cell γ detector (Bioscan), and a PC with Shimadzu Class VP 7.2 software used for system control.

$^{11}CO_2$ was produced through the $^{14}N(p,\alpha)^{11}C$ nuclear reaction by bombardment of a high-pressure target containing a mixture of nitrogen and oxygen (0.5%–1%) with a 16.8-MeV proton beam that was produced by the PETTrace cyclotron (GE Healthcare) cyclotron. $^{11}C$-Methyl iodide was synthesized by the gas-phase method from $^{11}CO_2$ using the FXMeI or the FXC module (GE Healthcare), by initially converting $^{11}CO_2$ to $^{11}C$-methane, followed by reaction of $^{11}C$-methane with iodine at 720 °C (*(2)*).

Radiolabeling of $^{11}C$-UCB-J **7** was performed by initially trapping $^{11}C$-methyl iodide in a degassed and acetone/ice bath cooled solution of 0.3-0.4 mg of tris(dibenzylideneacetone)-dipalladium(0) ($Pd_2(dba)_3$), 0.4-0.5 mg of tri(*o*-tolyl)-phosphine (P(*o*-tol)$_3$), and 0.4-1 mg potassium carbonate in 8:1 *N*,*N*-dimethylformamide (DMF)/water (v/v, 250 µL). After the radioactivity peaked, the solution was stirred for 3 min at ambient temperature and the solution of 1-1.2 mg precursor **6** in 100 µL of 8:1 DMF/water was added. The reaction mixture was then heated for 5 min at 100 ºC.

The reaction solution was cooled in an acetone/ice bath, then diluted with 1.6 mL of 1 N HCl and filtered through a 0.45 µm membrane filter (13 mm Millex-HV PVDF), and then loaded to a Gemini-NX C18 preparative HPLC column (5 µm, 10 × 250 mm) for purification. The column was eluted with acetonitrile/0.1 M ammonium formate /saturated ammonium hydroxide (35:65:1.3, v/v, aq. phase pH ~10) at a flow rate of 2 mL/min for the first 3 min, and 5 mL/min thereafter. The desired radioactive product fraction was collected, diluted with 50 mL of de-ionized (DI) water, and passed through a Waters C18 Classic SepPak cartridge. The SepPak cartridge was rinsed with 10 mL of

0.001 N HCl. The radioactive product was recovered by eluting the SepPak with 1 mL of absolute ethanol (USP), followed by 3 mL of saline (USP), into a product vial containing 7 mL of saline (USP) and 40 μL of 4.2% sodium bicarbonate (USP). This solution mixture was then passed through a sterile membrane filter (0.22 μm) for terminal sterilization and collected in an empty sterile vial to afford a formulated solution ready for dispensing and administration. The chemical purity, radiochemical purity, and specific activity of $^{11}$C-UCB-J were determined by HPLC analysis of the product solution (column: Genesis C18, 4.6 × 250 mm, 5 μm; mobile phase: 38% acetonitrile and 62% 0.1 M aqueous ammonium formate with 0.5% acetic acid (v/v, pH 4.2); flow rate: 2 mL/min; ultraviolet detector wavelength: 261 nm). The identity of $^{11}$C-UCB-J was confirmed by coinjection of the product with the unlabeled UCB-J. The radiolabeled product and UCB-J coeluted from the analytic HPLC column. The enantiomeric purity of $^{11}$C-UCB-J was also verified by analytic chiral HPLC by coinjection with the unlabeled reference standard **3** (Supplemental Fig. 4).

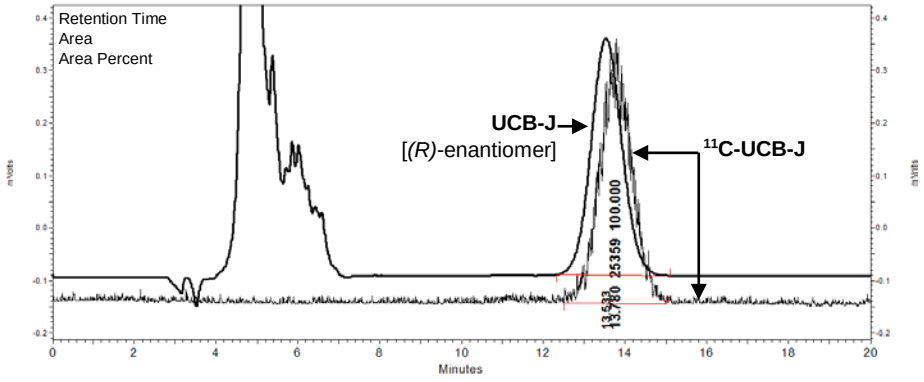


**Supplemental F**igure 4. Analytical chiral HPLC chromatograms of $^{11}$C-UCB-J coinjection with the reference standard.

**In vitro binding assays**

Reagents and reference compounds used were of analytical grade and obtained from various commercial sources. All cell culture reagents were obtained from Invitrogen (Merelbeke, Belgium). Radioligands ($^3$H-UCB30889, 1,184 GBq/mmol; $^3$H-UCB1418435, 925 GBq/mmol; and $^3$H-UCB101275-1, 1,110 -1,480 GBq/mmol) were obtained from G.E Healthcare, Amersham, U.K (now Perkin Elmer, Zaventem, Belgium) and reference compounds (levetiracetam, UCB108649-1 and UCB101275-1) were custom synthesized and stored according to manufacturer's recommendations. Test and reference compounds were dissolved in 100% DMSO or $H_2O$ to give 1 or 10 mM stock solution. Final DMSO concentration in assays was 0.1% unless otherwise stated.

Cell lines generated at UCB Biopharma were human embryonic kidney (HEK) 293 cells expressing human SV2A, SV2B or SV2C proteins or rat SV2A proteins. Cells were cultured in Dulbecco's Modified Eagle medium. The culture medium was supplemented with foetal bovine serum (FBS, 10%), 2 mM l-glutamine, 50 to 100 U/mL penicillin, 50 to 100 µg/mL streptomycin, and 200 µg/mL hygromycin B. Cells were grown at 37 °C with 95% air. Confluent cells were detached by 10 min incubation at 37 °C in phosphate buffered saline (PBS) containing 0.02% EDTA. Culture flasks were washed with 15 mL of ice-cold PBS. The cell suspension was centrifuged at 1,500 × *g* for 10 min at 4 °C. The pellet was homogenized in 15 mM Tris-HCl buffer (pH 7.5) containing 2 mM $MgCl_2$, 0.3 mM EDTA, 1 mM EGTA (buffer A) using a glass/teflon homogenizer. The crude homogenate was subjected to a freeze and thaw cycle in liquid nitrogen and DNAse (1 µL/mL) was then added. The homogenate was further incubated for 10 min at 25 °C before being centrifuged at 40,000 × *g* for 25 min at 4 °C. The pellet was re-suspended in

buffer A and washed once under the same conditions. The final crude membrane pellet was re-suspended at a protein concentration of 1-3 mg/mL in 7.5 mM Tris-HCl buffer (pH 7.5 at 25 °C) containing 250 mM sucrose and stored in liquid nitrogen until use. Membranes were incubated in binding buffer (see Suppl Table 1) containing test compound or positive control in the presence of the radioligand. The non-specific binding (NSB) was defined as the residual binding observed in the presence of a high concentration (1000 fold its $K_i$) of a specific unlabeled reference compound. Membrane-bound and free radioligands were separated by rapid filtration through glass fiber filters (GF/C). Samples and filters were rinsed by at least 6 mL of washing buffer. The entire filtration procedure did not exceed 10 seconds per sample. The radioactivity trapped on the filters was counted by liquid scintillation in a ß-counter. To determine the affinity of a compound for a given target, competition curves were performed with at least 10 concentrations of compound spanning at least 5 log units.

Supplemental Table 1. Details of in vitro binding assay determination

| | **hSV2A assay** | **hSV2B** | **hSV2C** |
|---|---|---|---|
| **Binding buffer** | 50 mM Tris-HCl (pH7.4) containing 2 mM $MgCl_2$ | | |
| **Filtration buffer** | Ice-cold 50 mM Tris-HCl (pH 7.4) | | |
| **Incubation time** | 120 min at 37 °C in 0.5 mL | 120 min at 37 °C in 0.5 mL | 120 min at 37 °C in 0.2 mL |
| **Radioligand** | $^{3}$H-UCB30889 (4 nM) | $^{3}$H-UCB1418435 (8 nM) | $^{3}$H-UCB101275-1 (20 nM) |
| **Proteins** | 75-125 µg HEK293 membranes | 2-5 µg HEK293 membranes | 40-60 µg HEK293 membranes |
| **Blocking drug** | Levetiracetam (1 mM) | UCB108649-2 (10 µM) | UCB101275-1 (100 µM) |

The selectivity of UCB-J was assessed by its ability to interact with various receptors, transporters, enzymes and ion channels (55 targets; Suppl Table 2) when tested at a concentration of 10 µM. Details of the binding procedures (protocol references) used at CEREP are available on their website.

Supplemental Table 2. Results of in vitro selectivity binding assay determination

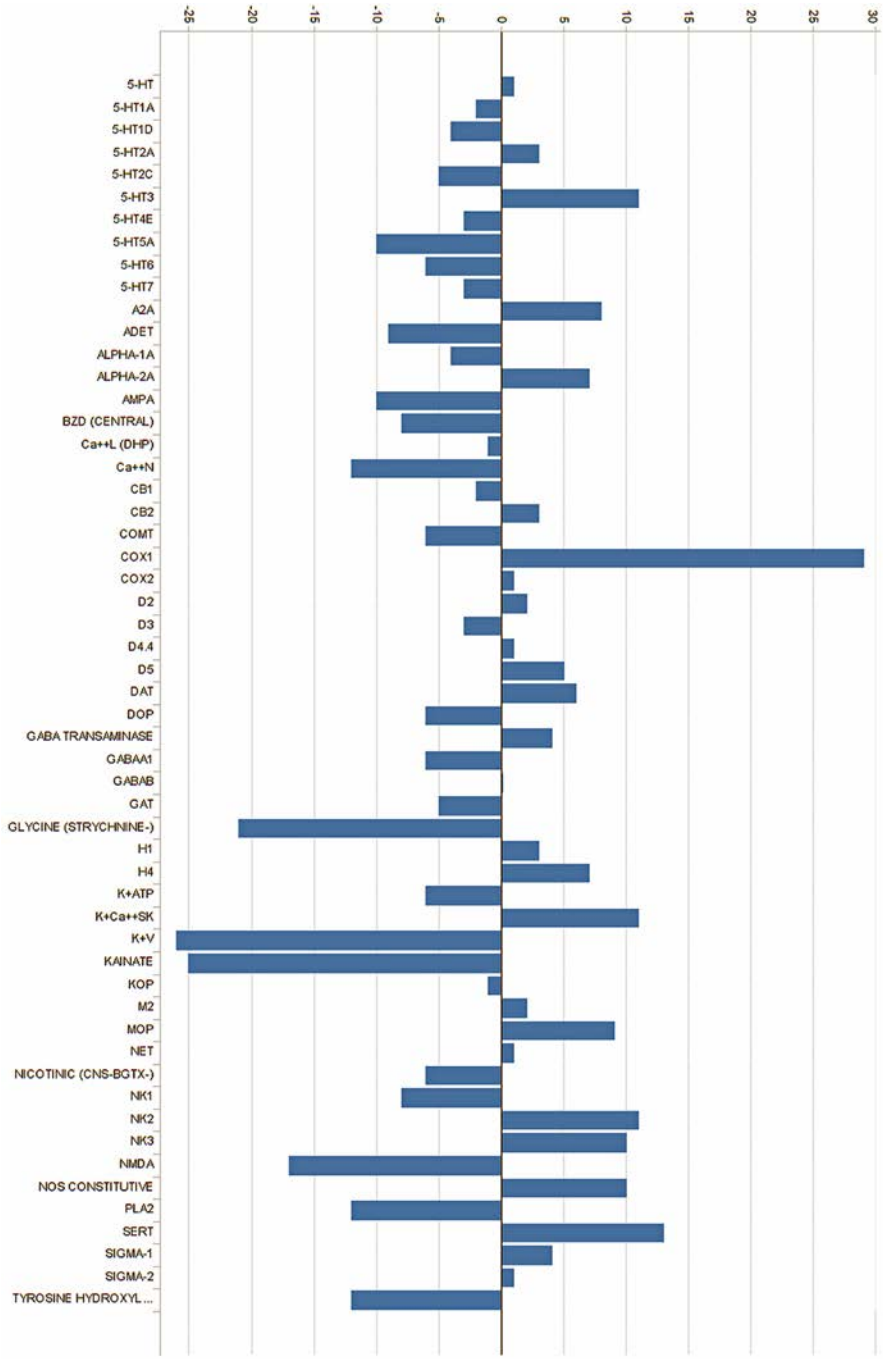

**In vitro and in vivo metabolism in rats**

Studies characterizing the pharmacokinetics, distribution, and metabolism of UCB-J included *in vitro* experiments, *in vivo* plasma pharmacokinetics, brain distribution, and metabolite profiling in rat plasma and brain are summarized in Table 1. The concentrations of UCB-J in biological matrices were determined by liquid chromatography electrospray ionization tandem mass spectrometry (LC/ESI-MS/MS). The qualitative analysis of the major metabolites present in rat plasma and brain samples following iv administration of 1 mg/kg UCB-J was performed on an ultra-performance liquid chromatography tandem mass spectrometry (UPLC/MS/MS) system. HPLC conditions are summarized in Suppl Table 3 and representative chromatograms of a rat plasma and brain sample are depicted in Suppl Figure 5.

Supplemental Table 3. UPLC conditions for the identification of UCB-J *in vivo* metabolites

| | |
|---|---|
| Mobile Phase A: | Water UPLC Quality Biosolve- ammonium acetate 10 mM / Acetic Acid (100/0.1%) |
| Mobile Phase B: | Acetonitrile ULC Quality Biosolve |
| Gradient: | Time (min)/ Solvent A (%): 0.0/98; 1.0/98;9/10; 10.5/90; 10.51/98 |
| Flow Rate: | 0.40 mL/min |
| Injection Loop: | 100µL |
| Analytical Column: | Waters HSS-C18 (100 × 2.1 mm 1.8 µm) |
| PDA Scanning: | 210 to 400 nm |

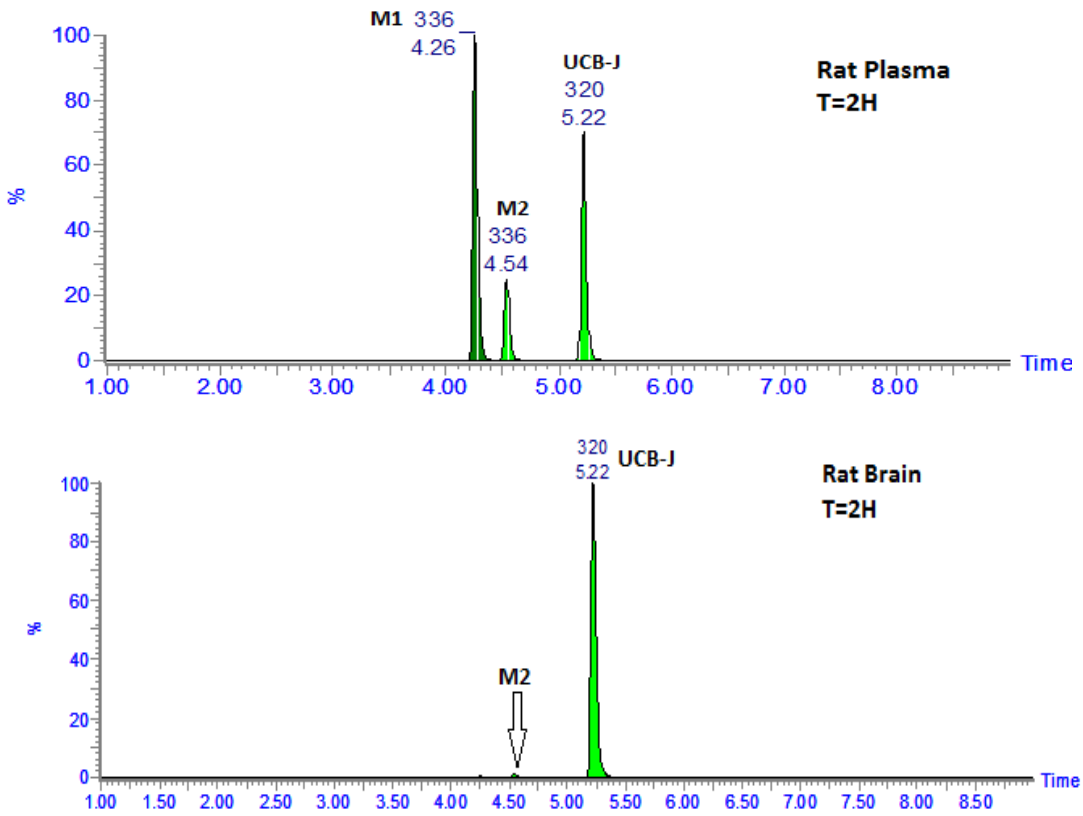


Supplemental Figure 5. Representative UPLC chromatograms of a rat plasma and brain sample

The permeation rate of UCB-J through Caco-2 cell monolayers was investigated in the apical-to-basolateral (A>B) and the basolateral-to-apical (B>A) directions. Apparent permeability ($P_{app}$) was expressed in nm/s. The *in vitro* binding of UCB-J to brain homogenate and plasma proteins was investigated in rat and human (plasma only), using the equilibrium dialysis method. The *in vitro* metabolic stability and interspecies metabolism of UCB-J were investigated in liver NADPH-fortified microsomes from mouse, rat, monkey and human. Parent drug disappearance was measured over 6 time points up to 40 min and intrinsic clearance was expressed in µL/min/mg protein.

**Metabolite Analysis, Arterial Input Function and Log *D* Determination**

Arterial blood samples were collected at various intervals to measure the plasma input function. In addition, arterial blood samples at 3, 8, 15, 30, 60 and 90 min after tracer injection were collected (Suppl Fig. 6.B), processed and analyzed for unmetabolized parent fraction with automatic column-switching HPLC system (3) equipped with a capture column (19 x 4.6 mm) packed with Phenomenex SPE C18 Strata-X sorbent (Torrance, CA, USA) eluting with 1% acetonitrile and 99% water (v/v) at a flow rate of 2 mL/min, and a Phenomenex Gemini-NX C18 analytical column (5 µm, 250 x 4.6 mm) eluting with 40% acetonitrile and 60% 0.1 M ammonium formate (v/v) at a flow rate of 1.6 mL/min. HPLC eluate was fraction-collected in 2 min intervals and the fractions were measured with gamma well counters (Wizard 1480/ 2480, Perkin Elmer, Waltham, MA, USA). The sample recovery rate, extraction efficiency, and HPLC fraction recovery were monitored by measuring radioactivity in the plasma, plasma filter, plasma filtrate, and HPLC fractions. The unmetabolized parent fraction was determined as the ratio of the radioactivity corresponding to the parent (retention time of ~ 11 min, Suppl Fig. 6.A) to the total amount of radioactivity collected, normalized to the recovery rate, which was determined by corresponding reference plasma samples and fitted with a bounded sum of exponential function. The arterial plasma input function was calculated as the product of the plasma time activity curve (TAC) and the parent fraction curve.

Plasma free fraction ($f_p$) was measured by the ultrafiltration method in triplicate using Millipore Centrifree® micropartition device (4104, Billerica, MA, USA) and with 3 mL of arterial blood sample taken immediately prior to tracer injection. The free fraction $f_p$ was determined as the radioactivity ratio of the ultrafiltrate to plasma.

Log *D* was determined by the modified method from previously published procedures (*(4)*). $^{11}$C-UCB-J (1 MBq) was added to a 2.0 mL microtube containing 0.8 mL 1-octanol and 0.8 mL 1X Dulbecco's phosphate buffered saline (PBS, pH=7.4). The mixture was vigorously vortexed for 20 s and centrifuged at 2,000 *g* for 2 min. A subsample of the octanol (0.2 mL) and PBS (0.7 mL) layers was countered in a gamma counter. The major portion of the octanol layer (0.5 mL) is diluted with 0.3 mL octanol and mixed with a fresh portion of 0.8 mL PBS. The distribution coefficient log *D* was determined by the ratio of activity in octanol and PBS. Value of log *D* was determined to be 2.53 ± 0.02 (n=9).

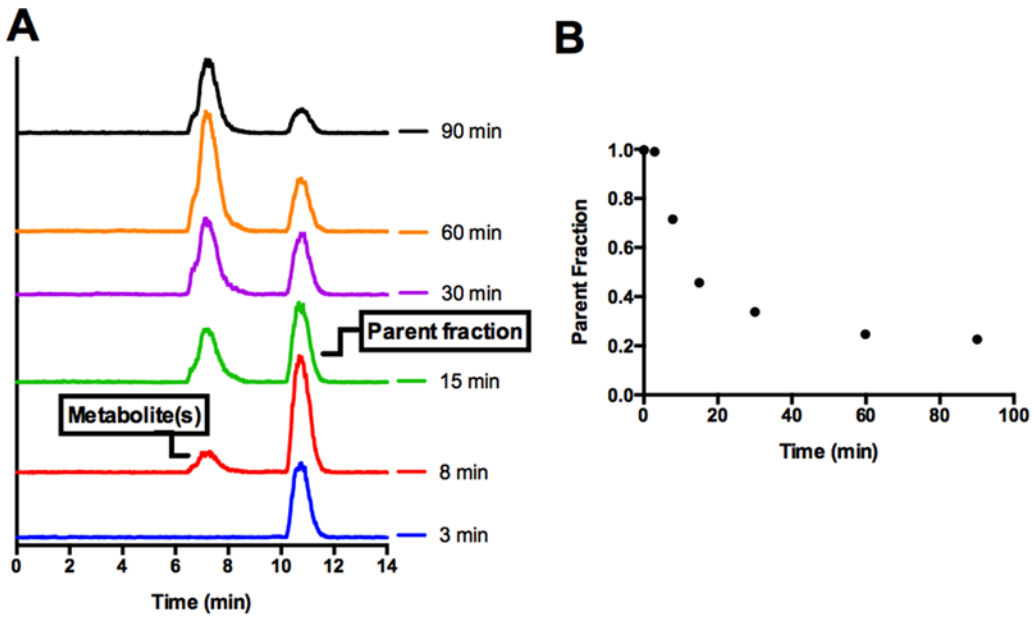


**Supplemental Figure 6**. A: Typical HPLC profile for $^{11}$C-UCB-J metabolite analysis; B: Representative baseline parent fraction curve.

**Modeling**

Multilinear Analysis (MA1) (*(5)*) with $t^*$= 40 min was also applied in conjunction with 1T for comparison purposes. Regional $V_T$ values are highly correlated between the 2 modeling methods, as shown in Supplemental Figure 7.

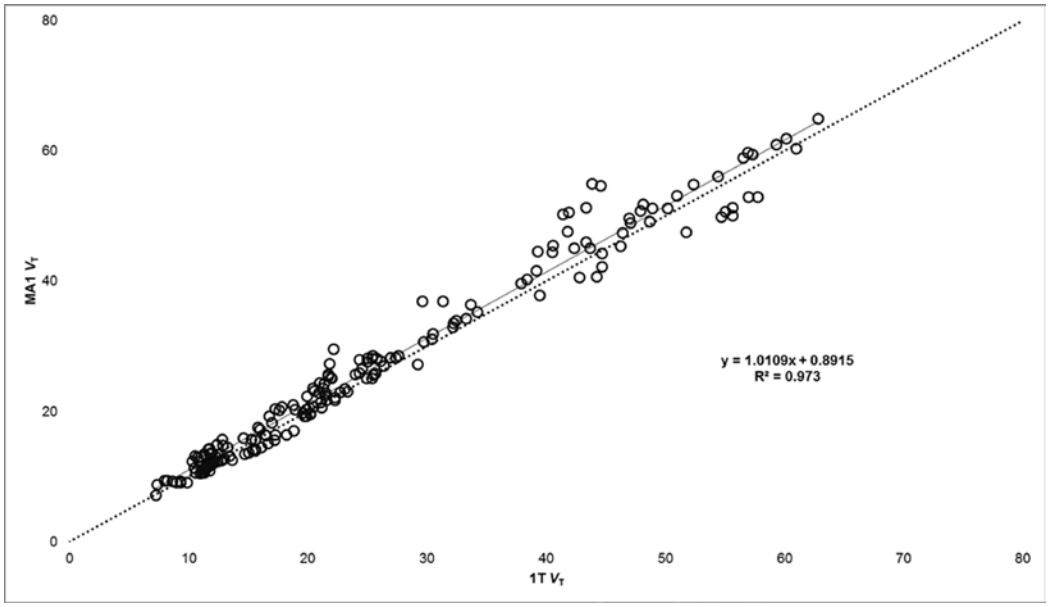


**Supplemental Figure 7**. Comparison of $V_T$ values from 1T and MA1 analyses.

**Definition of a reference region**

As expected, there was no evidence of a suitable reference region, i.e., one without specific binding in gray matter regions. We evaluated the potential utility of the white matter (WM), specifically the centrum semiovale (CS), by analysis of 4 scans from the *in vivo* $K_d$ study, performed in one animal. These included one baseline scan with injection of $^{11}$C-UCB-J only, and 3 scans with co-injection of $^{11}$C-UCB-J with 17, 50, and 150 µg/kg of UCB-J. Ideally, the $V_T$ values in the WM would not be affected by co-injection

with UCB-J. However, a challenge in using WM in rhesus monkey is the partial volume effect (PVE), especially given the high contrast between gray matter (GM) and WM. Thus a partial volume correction (PVC) was performed as follows.

First, a rectangular bounding box (12 slices) was defined in the neighborhood of the CS. Within this box, a GM mask was defined manually on the animal's MR scan. A CSF mask was determined by a segmentation algorithm. The remaining voxels in the brain within this box were designated as the WM mask. This mask was smoothed to simulate the partial volume effect, and a CS ROI was chosen by picking the voxels with the highest WM membership, i.e., the highest values in the smoothed mask image. This ROI had a volume of ~ 0.5 mL. The CS ROI was applied to 1T $V_T$ parametric images from the *in vivo* $K_d$ study, and the uncorrected $V_T$ values ranged from 21.9 mL·cm$^{-3}$ in the baseline scan down to 8.6 mL·cm$^{-3}$ for the self-blocking scan with a high dose of $^{1}$UCB-J (150 μg/kg).

Correction for partial volume between GM and WM regions was performed in a manner similar to that of Rousset et al (*(6)*). Results were found to be sensitive to the value of FWHM used in the correction. Assuming a Gaussian point spread function with FWHM of 3.5 or 3.75 mm (based on point source data reconstructed with the same algorithm and filter), smoothed mask images were used to calculate spill-over and recovery coefficients. The corrected CS $V_T$ values were 7.1±1.1 mL·cm$^{-3}$ (baseline scan: 8.7 mL·cm$^{-3}$, high-dose self-blocking scan: 7.0 mL·cm$^{-3}$) for FWHM of 3.5 mm, and 6.1±0.7 (baseline scan: 6.5 mL·cm$^{-3}$, high-dose self-blocking scan: 6.7 mL·cm$^{-3}$) for FWHM of 3.75 mm. These latter

values show that a corrected CS $V_T$ value is in excellent agreement with $V_{ND}$ of GM regions derived from the occupancy plots (6.3 ± 0.6 mL·cm$^{-3}$). Thus, these PVC results strongly support the potential utility of a CS region as a suitable reference region for $^{11}$C-UCB-J.

**Comparison of $^{11}$C-UCB-J and $^{18}$F-UCB-H**

Studies in rhesus monkeys were also performed with $^{18}$F-UCB-H, which like $^{11}$C-UCB-J, demonstrated reversible kinetics and binding blockade by levetiracetam. To assess which tracer has higher specific binding ($BP_{ND}$), we applied a graphical method (*7*) that plots $V_T$ of one tracer vs. the other (Suppl Fig. 8). The positive y-intercept of the regression line means that $^{11}$C-UCB-J has higher $BP_{ND}$ than $^{18}$F-UCB-H.

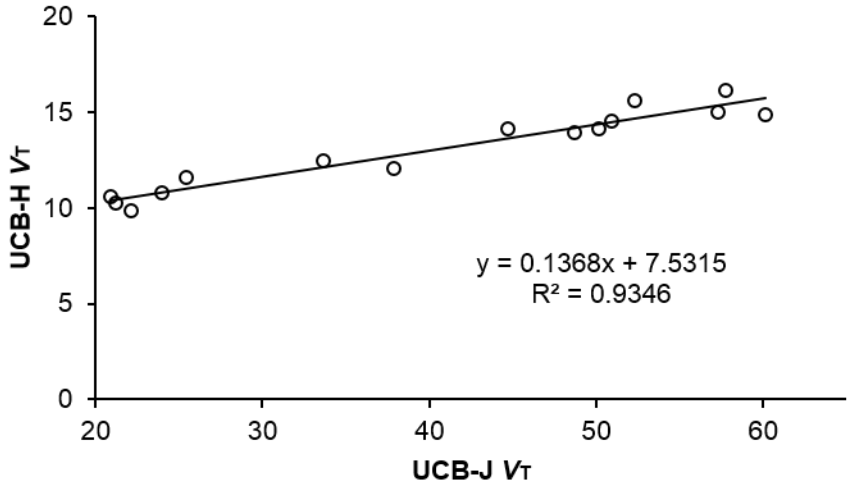


Supplemental Figure 8. Comparison of $V_T$ values between $^{18}$F-UCB-H and $^{11}$C-UCB-J across regions

Based on the mathematical interpretation of the intercept (*7*), we can conservatively estimate that the fractional increase in $BP_{ND}$ of $^{11}$C-UCB-J vs. $^{18}$F-UCB-H is at least 3, i.e., if $^{18}$F-UCB-H had a $BP_{ND}$ value of 1, $^{11}$C-UCB-J would have a $BP_{ND}$ value of 4. Further, using the mathematical interpretation of the slope (0.14), and correcting for the difference in $f_P$ between tracers, it was estimated that $^{11}$C-UCB-J has a 9-fold higher *in vivo* affinity for SV2A than $^{18}$F-UCB-H. This difference is consistent with the *in vitro* affinity of the two compounds for human recombinant SV2A at 37°C: 6 and 40 nM, respectively, for UCB-J and UCB-H.

This between-tracer difference in $BP_{ND}$ can explain the variation in the blocking effect of levetiracetam between $^{11}$C-UCB-J and $^{18}$F-UCB-H. levetiracetam at a dose of 10 mg/kg produced ~ 60% occupancy with $^{11}$C-UCB-J in rhesus monkey, while the same dose produced 26% reduction in $V_T$ with $^{18}$F-UCB-H in rat (*8*). A dose of 30 mg/kg produced 90% occupancy with $^{11}$C-UCB-J, whereas a dose of 100 mg/kg produced 44% reduction in $V_T$ with $^{18}$F-UCB-H. A smaller $BP_{ND}$ value will result in a lower percent reduction in $V_T$ at a given occupancy level.

Another potential contributing factor to the variation in the blocking effect of levetiracetam between $^{11}$C-UCB-J and $^{18}$F-UCB-H is the difference in the timing of drug administration. In the experiments described here, levetiracetam was given ~2.5 h before injection of $^{11}$C-UCB-J, while in the experiments in rat, the drug was given at 15 min before the PET scan (*8*). Because levetiracetam penetrates the brain very slowly (Nicolas et al., under review), administration of levetiracetam 15 min before tracer injection would not measure the maximum occupancy produced by a given dose. To confirm this, we

performed 2 PET scans with $^{18}$F-UCB-H where levetiracetam (10 mg/kg) was given 2.5 h before the PET scan, and the occupancy produced was ~80% (data not shown).

**REFERENCES**

**1.** Mercier J, Archen L, Bollu V, et al. Discovery of Heterocyclic Nonacetamide Synaptic Vesicle Protein 2A (SV2A) Ligands with Single-Digit Nanomolar Potency: Opening Avenues towards the First SV2A Positron Emission Tomography (PET) Ligands. *ChemMedChem.* 2014;9:693-698.

**2.** Larsen P, Ulin J, Dahlstrøm K, Jensen M. Synthesis of [11C]iodomethane by iodination of [11C]methane. *Applied Radiation and Isotopes.* 1997;48:153-157.

**3.** Hilton J, Yokoi F, Dannals RF, Ravert HT, Szabo Z, Wong DF. Column-switching HPLC for the analysis of plasma in PET imaging studies. *Nuclear Medicine and Biology.* 2000;27:627-630.

**4.** Del Rosario RB, Jung Y-W, Baidoo KE, Lever SZ, Wieland DM. Synthesis and in vivo evaluation of a 99m 99Tc-DADT-Benzovesamicol: a potential marker for cholinergic neurons. *Nuclear Medicine and Biology.* 1994;21:197-203.

**5.** Ichise M, Toyama H, Innis RB, Carson RE. Strategies to improve neuroreceptor parameter estimation by linear regression analysis. *J Cereb Blood Flow Metab.* 2002;22:1271-1281.

**6.** Rousset OG, Collins DL, Rahmim A, Wong DF. Design and implementation of an automated partial volume correction in PET: application to dopamine receptor quantification in the normal human striatum. *J Nucl Med.* 2008;49:1097-1106.

**7.** Guo Q, Owen DR, Rabiner EA, Turkheimer FE, Gunn RN. A graphical method to compare the in vivo binding potential of PET radioligands in the absence of a reference region: application to [(1)(1)C]PBR28 and [(1)(8)F]PBR111 for TSPO imaging. *J Cereb Blood Flow Metab.* 2014;34:1162-1168.

**8.** Warnock GI, Aerts J, Bahri MA, et al. Evaluation of 18F-UCB-H as a Novel PET Tracer for Synaptic Vesicle Protein 2A in the Brain. *J Nucl Med.* 2014;55:1336-1341.